Quantifying asymmetry in non-symmetrical morphologies, with an example from Cetacea

*Ellen. J. Coombs[1,2]

Ryan. N. Felice[2,3]

1. Department of Genetics, Evolution, and Environment, University College London, London, UK
2. Department of Life Sciences, The Natural History Museum, London, UK
3. Centre for Integrative Anatomy, Department of Cell and Developmental Biology, University College London, London, UK

*corresponding author: Ellen Coombs, Department of Genetics, Evolution, and Environment, University College London, London, UK, ellen.coombs.14@ucl.ac.uk

Running headline: Quantifying shape in non-symmetrical morphologies

Abstract

1. Three-dimensional measurements of morphology are key to gaining an understanding of a species' biology and to answering subsequent questions regarding the processes of ecology (or palaeoecology), function, and evolution. However, the collection of morphometric data is often focused on methods designed to produce data on bilaterally symmetric morphologies which may mischaracterise asymmetric structures.

2. Using 3D landmark and curve data on 3D surface meshes of specimens, we present a method for first quantifying the level of asymmetry in a specimen and second, accurately capturing the morphology of asymmetric specimens for further geometric analyses.

3. We provide an example of the process from initial landmark placement, including details on how to place landmarks to quantify the level of asymmetry, and then on how to use this information to accurately capture the morphology of asymmetric morphologies or structures. We use toothed whales (odontocetes) as a case study and include examples of the consequences of mirroring landmarks and curves, a method commonly used in bilaterally symmetrical specimens, on asymmetric specimens.

4. We conclude by presenting a step-by-step method to collecting 3D landmark data on asymmetric specimens. Additionally, we provide code for placing landmarks and curves on asymmetric specimens in a manner designed to both save time and ultimately accurately quantify morphology. This method can be used as a first crucial step in morphometric analyses of any biological specimens by assessing levels of asymmetry and then if required, accurately quantifying this asymmetry. The latter not

only saves the researcher time, but also accurately represents the morphology of asymmetric structures.

Keywords: asymmetry, geometric morphometrics, landmarks, morphology

Introduction

In recent years there has been a rapid advance in the collection and accumulation of rich morphological data sets using computer tomography (CT) and surface scanning (Davies et al., 2017). High quality data has in turn driven the demand for new methods which accurately and comprehensively capture and represent organismal morphology (Goswami et al., 2019). One such method, geometric morphometrics, often involves the use of 2D or 3D coordinates (landmarks) that are placed on the surface of a specimen or morphology and used to quantify shape independent of isometry, position, and rotation (Bookstein 1991; Zelditch et al. 2004; Lawing and Polly 2010; Adams et al. 2013; Bardua et al., 2019a). Quantifying morphology using these geometric morphometric methods has a long history, and the last few decades in particular has seen an explosion of new advances now used across the biological sciences (Lawing and Polly, 2010; Adams et al., 2013; Bardua et al., 2019a).

In addition to 2D and 3D fixed landmarks, many studies now use semi-landmarks to capture the shape of the regions that fall between landmarks (Gunz et al., 2005; Gunz and Mitteroecker 2013). Semi-landmarks are used to define the outline of structures, such as sutures or ridges, or even entire surfaces, and can provide a significant increase in the shape captured compared to using just landmarks alone (Bookstein, 1991). Curve semi-landmarks (hereafter referred to as ‘curves’ or ‘semi-landmarks’) have been used successfully to quantify a vast array of

organismal morphology, including green algae (*Halimeda tuna*: Neustupa and Nemcova, 2018), bird beaks (Cooney et al., 2017), and cranial morphology (Bardua et al., 2019b, Felice et al., 2020). Their use expands the quantification of shape to include the morphology of outlines (e.g., bone margins or veins) and ridges (Cooney et al., 2017; Bardua et al., 2019a). There are numerous reviews which cover the costs and benefits of landmarks alone vs. including semi-landmarks as well as surface semi-landmarks and automated landmarks (see Bardua et al., 2019a).

Coordinate data for structures such as the skull, which is generally bilaterally symmetrical in most species, often comprise landmarks placed on one side of the structure. This is done for several reasons. First, by landmarking only one side and then mirroring those landmarks to the other (symmetrical) side, the user greatly reduces the time required for data capture. Second, landmarking both sides of a symmetrical morphology can produce redundant shape information, but ultimately, using symmetrical data has been shown to improve superimposition (Cardini, 2016a; 2016b). To accommodate these issues, Bardua et al., (2019a) recommend imputation of the missing side through mirroring of the existing landmarks along a midline plane, then removing these mirrored landmarks after Procrustes superimposition (translation to a common origin, scaling to unit centroid size, and rotation to leave only shape data; Mitteroecker and Gunz, 2009) to reduce data dimensionality and redundant information. While this method has proven to work well in capturing the shape of bilaterally symmetrical morphologies (e.g., Adams et al., 2013; Dumont et al., 2016; Felice and Goswami, 2018; Bardua 2019b; Watanabe et al., 2019) into which most aspects of vertebrate anatomy fall, the same cannot be said for rarer asymmetrical morphologies (Fig. 1).

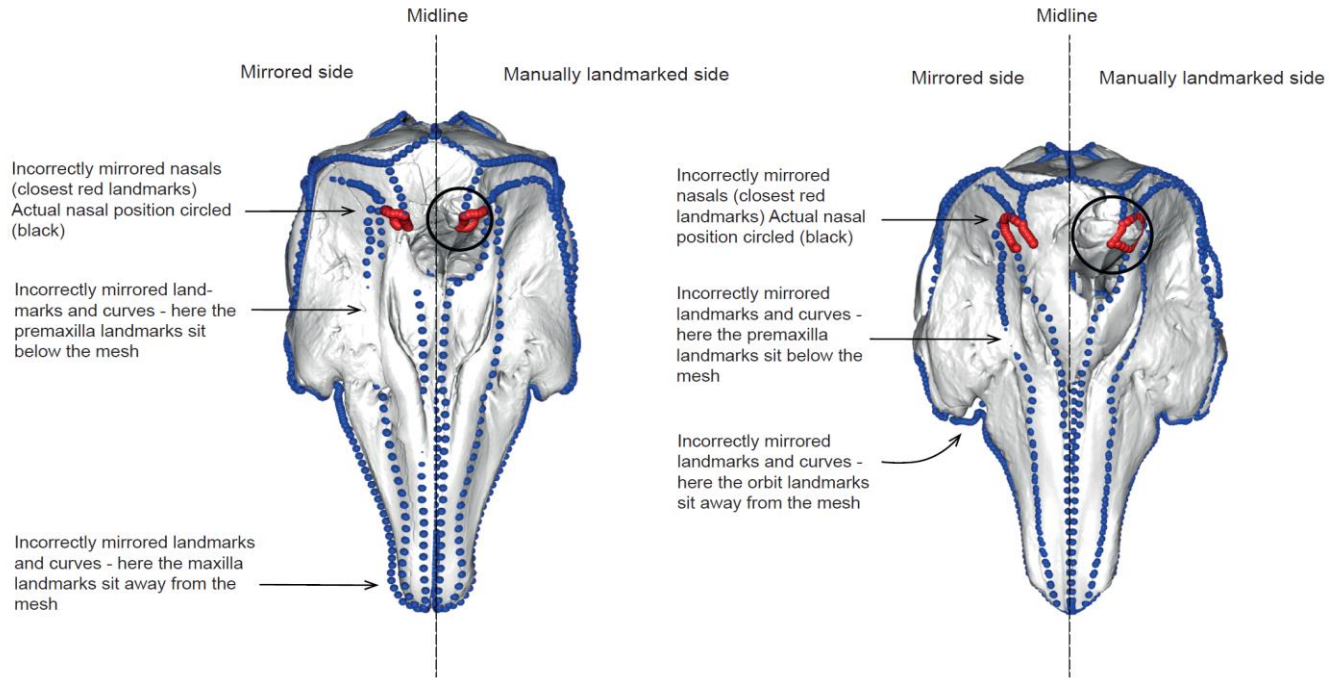

Fig. 1. Computer mirrored landmarks can misrepresent true morphology in asymmetric specimens. Landmarks and semi-landmarks are shown in blue on the skulls of two odontocetes. Nasal landmarks are shown in red to illustrate the inaccurate capture of the asymmetric morphology. Nasals and their actual positions are circled in black – ideally all red landmarks should sit within the black circle. Specimens shown are *Delphinapterus leucas* (USNM 305071, left) and *Monodon monoceros* (USNM 267959, right).

Asymmetrical morphologies

Symmetry in external morphology is the general rule among plants and animals, making the cases of directional asymmetry particularly interesting. However, it is now well known that some organisms do have a naturally occurring asymmetrical morphology. Directional asymmetry (DA), a type of asymmetry that occurs in a consistent direction between a pair of morphological structures, is often related to function or developmental morphology. This is typically expressed as size differences in bilaterally paired structures (e.g., limbs, muscles). This differs from

fluctuating asymmetry (FA) which is often used as a measure of stress in populations, of individual quality or of developmental instability (Graham et al., 1993; Klingenberg, 2003). FA is often minute and requires the capturing of measurement error on a different scale to the asymmetry covered in this study.

Directional asymmetry related to function is found across plants and animals with examples including the shells of turtles (yellow-bellied sliders (*Trachemys scripta scripta*); Parés-Casanova, 2020) and the appendicular skeleton of some cetaceans. In some cetaceans, the humerus and ulna is significantly larger on the right (dextral) side in the harbour porpoise (*Phocoena phocoena*) and the white-beaked dolphin (*Lagenorhynchus albirostris*) with a larger dextral muscle mass and higher mechanical stress indicating lateralized behaviours (Galatius, 2005; 2006). Handedness and associated directional asymmetry of limbs is also detected in humans (*Homo sapiens*; Auerbach and Ruff, 2006) and rhesus macaques (*Macaca mulatta*; Falk et al., 1998), and in the pectoral appendages or walruses (*Odobenus rosmarus*; Levermann et al., 2003). In some taxa, such as the fox (*Vulpes vulpes*), directional asymmetry in the limbs, skull, and pelvis is not associated with preferential use but instead with differential biases in growth (Kharlamova et al., 2010).

In contrast to these size-based examples of asymmetry, some taxa exhibit directional asymmetry in the morphology or position of paired structures. In owls (Strigiformes) (Krings et al., 2020), pronounced bilateral asymmetry in the external ears is related to directional hearing, or sound localization ability (Payne I97I; Norberg, 1977; Norberg 2002; Krings et al., 2020). Asymmetry in the owl ear (both soft tissues and temporal parts of the skull, including modifications in the neurocranium and cartilaginous elements; Krings et al., 2020), serves to make the

vertical directional sensitivity patterns different between the two ears for high frequencies, thus making possible vertical localization based on binaural comparison of intensity and spectral composition of sound (Norberg, 1977). Flatfishes (Pleuronectiformes) represent a diverse clade of benthic teleost fishes that possess a striking degree of cranial asymmetry exceeding that of any other vertebrate lineage (Black and Berendzen, 2020; Evans et al., 2021). The eyes of most flatfishes sit on the same side of the head; a development that happens during the larval stage where one eye of a symmetrical lava migrates to the other side. This produces a highly asymmetric cranium and has allowed the fish to colonise and dominate benthic aquatic habitats (Evans et al., 2021). Directional asymmetry is also widespread in invertebrates (see Okumura et al., 2008; Pélabon and Hansen, 2008), including wing size and shape (Klingenberg et al., 1998; Pélabon and Hansen, 2008), body shape (e.g., the Chilean magnificent beetle (*Ceroglossus chilensis*); Bravi and Benítez, 2013, and in the dextral spiralling of the shell in snails in the family Lymnaeidae; Okumuru et al., 2008), and eye morphology (e.g., cockeyed squids *Histioteuthis heteropsis* and *Stigmatoteuthis dofleini*; Thomas et al., 2017). Although it constitutes most of the examples in this study, directional asymmetry is by no means restricted to Animalia. Plants exhibit forms of asymmetry analogous to "handedness" in animals (Bahadur et al., 2019).

Simply, directional asymmetry is the natural condition for many taxa and avoiding the issue of left-right symmetry is not always an option if one wishes to accurately capture a specimen's morphology. Here, we use toothed whales (odontocetes) as an example to firstly calculate how much directional asymmetry is present, and second, ensure that asymmetry is accurately quantified. Toothed whales (odontocetes) are well-known to have asymmetrical crania (Ness, 1967;

Thompson, 1990; Fahlke et al., 2011; Churchill et al., 2018). This directional asymmetry is thought to have evolved as a result of an evolutionary hyperallometric investment into sound-producing soft tissue structures which have consequently driven evolution of the underlying bony structures, to facilitate high frequency vocalisation (echolocation) (Heyning and Mead, 1990). It is not entirely clear why the shift is sinistral (rather than dextral), but some propose it may be a by-product of selection pressure for a sinistrally positioned larynx and hyoid apparatus which provides a large, right piriform sinus whilst facilitating the swallowing of prey underwater (Macleod et al., 2007).

Examples such as these (and many others) underscore the apparent ubiquity of directional asymmetry in animals and plants, further bolstering our increasing knowledge of consistent left-right asymmetries (Klingenberg and McIntyre, 1998a; Klingenberg et al., 2002). Although an increasingly well-known natural aspect of function and sometimes developmental morphology in some taxa, directional asymmetry is not often considered during standard geometric morphometric analyses and instead may be underrepresented (Fig.1). Further, previous studies have successfully addressed quantifying variation among individuals and asymmetry (Klingenberg et al., 1998; Klingenberg et al., 2002; Klingenberg, 2015), generally by calculating the Procrustes distance between a shape and its reflection, offering a measure of asymmetry (Bookstein 1991; Klingenberg and McIntyre 1998b; Mitteroecker and Gunz, 2009). The protocol proposed here builds on these previous methods with a focus on the benefits of using landmarks and semi-landmarks and, importantly, allowing the user to create a universal landmarking scheme regardless of a specimens' asymmetry. This means symmetric and asymmetric specimens (for

example from different species, genera, or families) can be analysed in the same geometric morphometric workflow.

Finally, the time-consuming nature of manually applying landmarks and semi-landmarks can impose limitations on data collection and project scope. For this reason, researchers use automated (Boyer et al., 2015a; 2015b) and semi-automated (Schlager et al. 2019) approaches to geometric morphometrics. However, these methods are not applicable to all morphologies. We estimate that using the method presented here reduces per-specimen processing time by about one third compared to applying semi-landmark curves to the whole specimen.

Description

Standard geometric morphometric methods for mirroring landmarks and semi-landmarks ('curves') may misrepresent asymmetric specimens (Fig 1). Manually placing semi-landmarks on the entirety of an asymmetric specimen would provide a more accurate representation of the morphology; however, it is an extremely time-consuming solution. Here we offer a practical method for combining the two methods of manually landmarking and semi-landmarking asymmetric bones whilst mirroring bilaterally symmetrical bones. This method provides an accurate quantification of the morphology but also minimises the need and time taken to manually semi-landmark the entire specimen. We offer a solution for:

1. Quantifying asymmetry to determine whether landmarks should be manually placed rather than computer mirrored.
2. Using these data to create a landmarking protocol which will capture the morphology of both asymmetrical and symmetrical parts of the morphology,

while minimising the time needed to semi-landmark the entire specimen (i.e., minimising per specimen processing time).

3. Producing an accurate representation of the morphology to then carry out standard geometric morphometrics.
4. Creating a pipeline that ensures both bilaterally symmetrical specimens and asymmetric specimens can be compared in the same analyses. The number and location of landmarks and semi-landmark curves is identical, *only the method of placement of landmarks is different*. This results in a global landmark and curve configuration that is the same among specimens regardless of whether they are asymmetrical or not, important for taxa for which some but not all specimens may have asymmetric morphologies.

Alternatively, we recommend that researchers looking at known bilaterally symmetrical specimens carry out step 1 (using landmarks only) to ascertain whether there is in fact some asymmetry or deformation in the specimen and thus whether quantifying asymmetry or reassessment of the specimen is required. If no asymmetry is detected, the researcher is assured that their specimen is bilaterally symmetric or does not have pronounced deformation and that mirroring of landmarks and semi-landmarks is sufficient to capture morphology.

Materials and Methods

Specimens and scan data collection

We demonstrate this approach using an example data set of odontocete (toothed whale) skulls. The data set comprises 157 odontocete skulls (Supporting Information: Table S1), representing 21 families, which range in asymmetry from no marked natural asymmetry to high levels of naso-facial asymmetry (see Coombs et al., 2020). Bilaterally symmetric mysticete (baleen whale) skulls are also used to visually illustrate the placement of curves on a bilaterally symmetrical specimen within the same analyses.

To analyse 3D geometric morphometric data that covers the entire cranium (to illustrate the point of full skull coverage of landmarks in asymmetric specimens) sampling was limited by specimen completeness and preservation. Inclusion of fossil specimens was determined by the extent of deformation and missing data. This does not mean that this method cannot be used on specimens with missing structures – see Supporting Information: Section 1: *Missing and variably present bones* to see how we dealt with incomplete specimens. Around 43% of specimens, including some extant specimens, had missing data, which was concentrated in the pterygoid, palate, jugal, squamosal, and tip of the rostrum (See Supporting Information: Section 1: *Missing and variably present bones*). Specimens with obvious taphonomic or other deformation were excluded from further analysis. Sexual dimorphism was not considered in this study as many fossils lack data on sex. All specimens are adults except for *Mesoplodon traversii* (NMNZ TMP012996) which is a sub-adult.

We scanned skulls using a Creaform Go!SCAN 20 or Creaform Go!SCAN 50 handheld surface scanner, depending on the size of the skull. Scans were initially

cleaned, merged, and exported in ply format using VXElements v.6.0, and further cleaned and decimated in Geomagic Wrap software (3D Systems). We decimated models down to 1,500,000 triangles, reducing computational demands, while retaining sufficient detail for morphometric analysis. In many morphometric studies, it is possible to digitally reconstruct bilateral elements by mirroring across the midline plane if the skull (or object) is preserved on one side (Gunz et al., 2009; Gunz and Mitteroecker, 2013; Cardini et al., 2016 a, b). Due to a natural asymmetry occurring in the odontocete skull (Fahlke et al., 2011; Coombs et al., 2020), we limited mirroring to marginally damaged bones or easily mirrored missing bones only, where it was clear that mirroring would not mask asymmetric morphology. Elements were mirrored using the 'mirror' function in Geomagic Wrap (3D Systems). Skulls are used as the example throughout this study, but these methods could be used on any morphology as long as a midline is determined (see *Step 2: Quantifying asymmetry in the skull for details*).

This study focuses on how to capture the morphology of an asymmetric specimen. There are several general steps (i.e., not related to quantifying asymmetry specifically) that should be taken after *Step 4: Informing the curve protocol – which curves to manually place*, before mirroring curves. These additional steps have been highlighted here as a side note and are available in the detail in the Supporting Information: Section 1*: Additional steps before running geometric morphometric analyses* so as not to disrupt the ordering of the focus method of this paper; quantifying asymmetry.

These steps include:

- **Resampling**: As the placement of curves onto specimens is done manually points are likely not evenly placed along the bone. Curves are resampled to create even spacing between landmark points before being slid (see Supporting Information in Botton-Divet et al. 2016; Felice, 2020).
- **Sliding** the curves is the next crucial step, as equally spaced semi-landmarks should not (and cannot) be treated as optimally placed and the initial arbitrary placement of semi-landmarks can impose strong statistical artefacts (Gunz and Mitteroecker 2013; Bardua et al., 2019a).

These steps are not required for determining the placement of curves or in quantifying asymmetry but should be carried out once the curve protocol has been implemented. Code for these steps is provided in Felice (2020) and also via: https://github.com/EllenJCoombs/Quantifying_asymmetry

Morphometric data collection – quantifying asymmetry

Step 1: Landmarking protocol

The placement of landmarks is the first step. These landmarks are then used to quantify asymmetry in the skull (or chosen morphology) (see *Step 2: Quantifying asymmetry*).

The first step is to quantify if, where, and how much asymmetry is evident in the skull. To do this, we placed 123 landmarks (sliding semi-landmarks are employed in a later step – see *Step 4: Informing the curve protocol*) irrespective of evidence of asymmetry over the entire surface of the skull (i.e., both sides) using

303 Stratovan Checkpoint (Stratovan, Davis, CA, USA) (Fig. 2). We used the 'single
304 point' option to add fixed landmarks. Landmarks were defined by Type I (biology)
305 and Type II (geometry) (Bookstein, 1991; Bookstein, 1997) and were chosen to
306 capture clearly homologous positions, e.g., tripartite sutures. Dentition was not
307 landmarked. The landmark configuration for this data set is detailed in Fig.2 and
308 Supporting Information; Table S2.

309

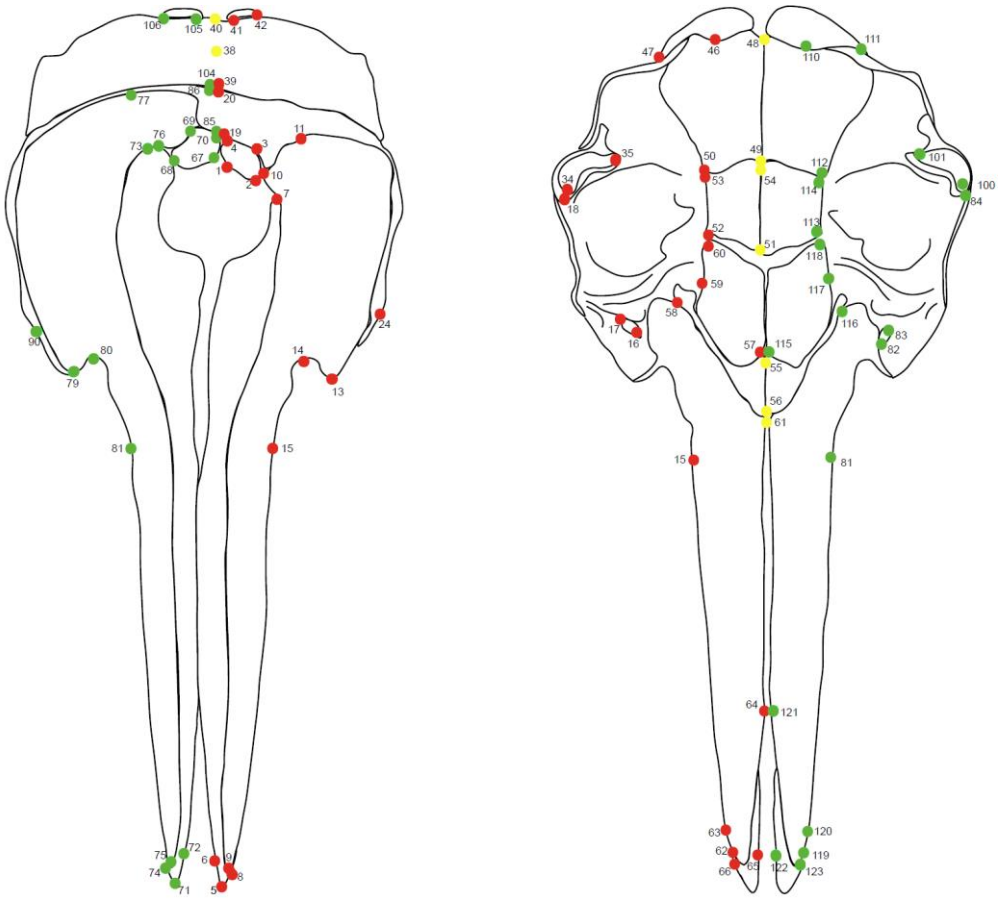

310

311 DORSAL VENTRAL

312

313

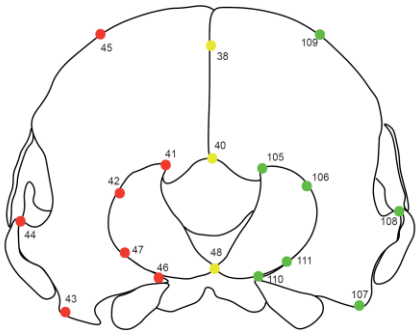

POSTERIOR

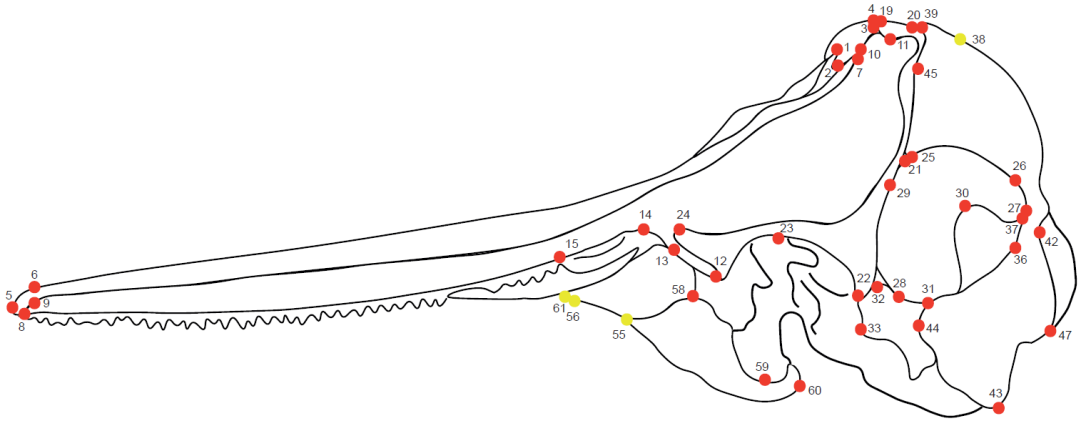

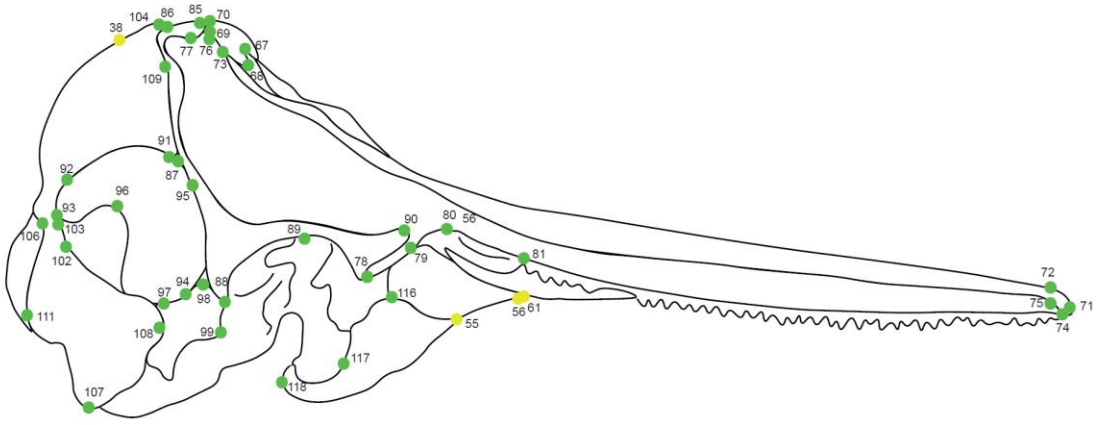

LATERAL

[Figure on previous page]

Fig. 2. Landmark configuration on the cetacean skull. Red landmarks are placed on the left-hand side (LHS) of the specimen, with corresponding green landmarks also *manually* placed on the right-hand side (RHS) of the specimen. Midline landmarks are shown in yellow. Numbers correspond to descriptions shown in the Supporting Information (Table S2).

Step 2: Quantifying asymmetry in the skull

Once a whole skull landmarking protocol has been formulated and added to specimens, the next step is to quantify where asymmetry occurs in the skull or morphology. This is so that landmarks and curves can be manually placed on these regions, rather than being mirrored by an automated procedure (hereafter referred to as computer mirroring, as can be done with bilaterally symmetrical structures). To do this, the protocol to quantify asymmetry as in Coombs et al., 2020 is followed. A brief summary of the methods is provided here and the code for quantifying asymmetry is available in detail at: https://github.com/EllenJCoombs/Quantifying_asymmetry

1. Manually place landmarks on the entirety of the specimen (i.e., left and right sides, Fig. 2), as described in *Step 1*.
2. Generate mirrored landmarks for one side of the skull. To mirror the landmarks, we used 9 midline landmarks as an anchor (yellow landmarks, Fig. 2). We used the `mirrorfill` function in the R package paleomorph v.0.1.4 (Lucas and Goswami, 2017). NB. We decided to mirror the left-hand landmarks because of chirality in cetaceans, i.e., nasals are sinistrally shifted. This will be organism specific, and consideration must be taken to ensure

specific morphologies are captured. In this example, mirroring the right-hand landmarks in cetaceans would exclude the nasals in some species. Consistency must be maintained between the side landmarks are mirrored from and to.

3. Compare the positions of the computer mirrored landmarks to those of the original, manually placed landmarks measuring the amount of landmark displacement between the two configurations.
4. Superimpose the specimens to remove all non-shape elements, i.e., size (scaling), translation, and rotation (positioning) from the data using Generalized Procrustes Analysis, here implemented in the `gpagen` function from the geomorph R package v.3.1.0 (Adams et al., 2019)
5. Calculate the Euclidean distances between a reference specimen (the computer-mirrored, landmarked specimen) (*Rn*) and a focal specimen (the manually landmarked specimen) (*Fn*). Both *Rn* and *Fn* are defined by three coordinates (*x*, *y*, *z*). The landmark displacements are measured for each landmark individually using the spherical coordinates system which measures between the n^{th} landmark of the *Fn* and the *Rn* specimens respectively, here implemented in the R package landvR v0.4 (Guillerme and Weisbecker, 2019).
6. If the specimen is asymmetric, the computer-mirrored landmark does not accurately reflect its morphology (Fig. 1). Estimate differences between *Fn* and *Rn* in the spherical coordinates system using the `coordinates.difference` function in landvR and extract the ρ (radius) for each landmark, for each specimen. This provides a measure of the Euclidean

distance between a manually placed landmark which accurately represents the specimen's morphology (*Fn)* and a computer -mirrored landmark (*Rn)*.

7. The larger the radii for a corresponding landmark the more displacement between *Fn* and *Rn.* We then interpret a higher *ρ* as an indication of more asymmetry in the skull (see Fig. 3 for a visualisation of this).

Step 3: Locating asymmetry in the skull or structure

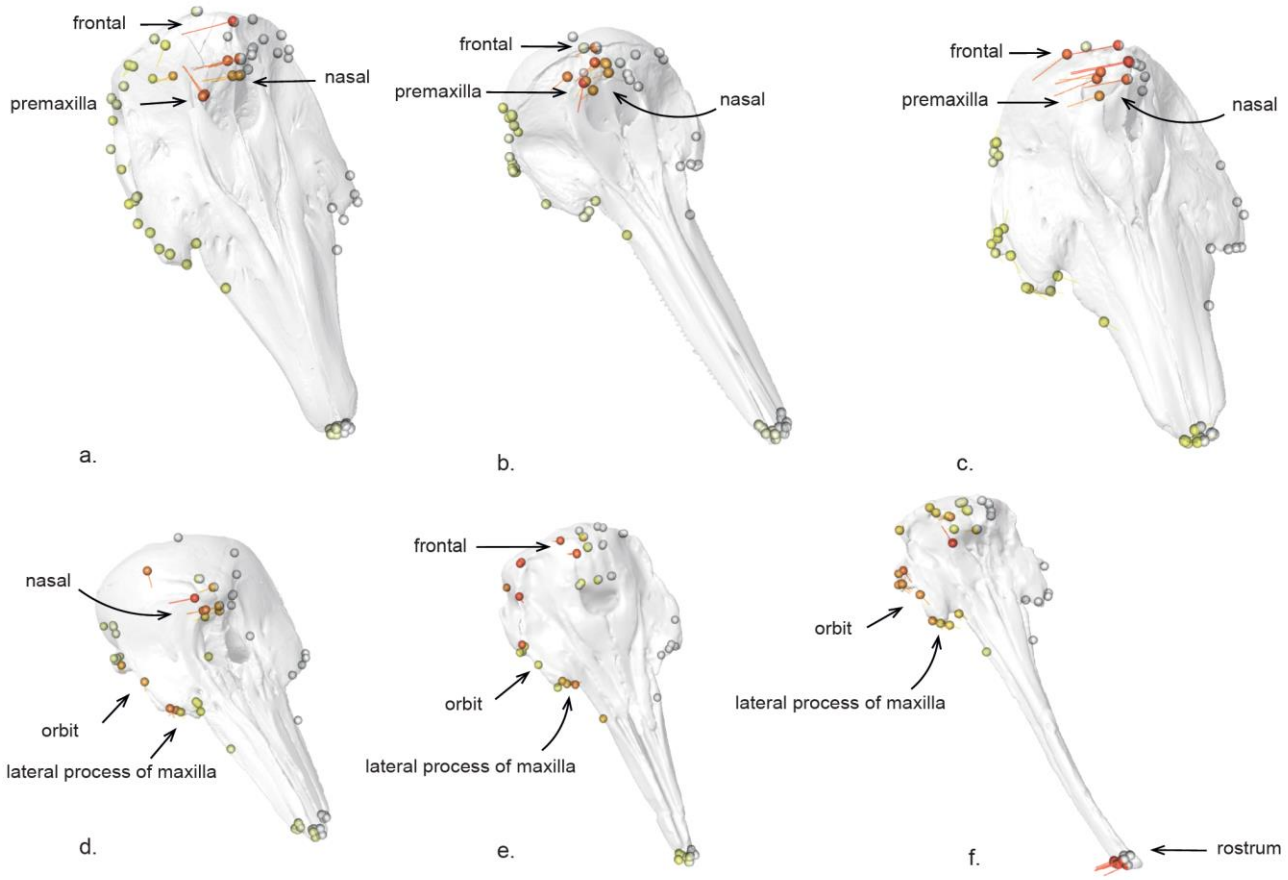

[Figure on previous page]

Fig. 3. Visualisation of *p* (radii) from landvR showing asymmetry in the toothed whale skull. Landmarks are shown on a mesh of the skulls. The white spheres (landmarks) on the landvR outputs show the *fixed* landmarks (1–66) on the left-hand side (LHS) of the skull. The landmarks on the RHS of the skull vary in colour depending on how much difference there is between a computer-mirrored landmark (*Rn*) (which assumes the skull is bilaterally symmetrical) and a manually placed landmark (*Fn*) (which accurately depicts asymmetry). The larger the difference between the computer-mirrored landmark and the manually placed landmark, the hotter the colour. The highest amount of asymmetry is shown in red and dark orange, less asymmetry is shown in pale orange and yellow. The tails coming from each of the landmarks show how much and in which direction the landmarks have moved from where the computer mirrored them, to where the landmarks sit when manually placed. Specimens a-c show most asymmetry in the frontal, nasal, and dorsal, posterior premaxilla as is common in many odontocetes and is associated with echolocation (see Coombs et al., 2020 for details). Specimens d-f show areas of asymmetry in the nasal and frontal (d and e) but also in the orbit, lateral process of the maxilla, and the tip of the rostrum (f). Some ventral landmarks are shown to assist with visual interpretation – landmarks shown are dependent on the specimen and orientation of that skull for illustration of the method only. Specimens: a. *Delphinapterus leucas* (USNM 305071), b. *Delphinus delphis* (AMNH 75332), c. *Monodon monoceros* (USNM 267959), d. *Phocoena spinipinnis* (NHM 1900.5.7.29), e. *Pliopontos littoralis* (SAS 193), f. *Tagicetus joneti* (IRSNB/RBINS M.1892). Not shown to scale.

Using landvR outputs for each of the specimens we can obtain a visual representation of where asymmetry occurs in the skull (Fig. 3) or structure. We recommend visualisation as a first step to ascertaining areas of asymmetry in the morphology. LandvR uses a ‘heat map’ approach to reflect displacement magnitude

as shown in Fig. 3 (see Weisbecker et al., 2019 and Viacava et al., 2020 for further examples). Generally, we advise focusing on landmarks with the hottest colours (red, dark orange) at the least and investigating them further to a) check they are logical and b) obtain a numerical measure of the magnitude of asymmetry.

We can obtain a numerical value for asymmetry (i.e., displacement) by pulling out the radius value for each landmark and further calculating an average radius value for each landmark across the data set. This allows us to determine which landmarks exhibit the highest asymmetry. We then identify landmarks with high asymmetry for manual landmarking as they are the ones most likely to be misrepresented by mirroring alone. In this data set, the highest landmarks of variation are shown in Table 1. Fig. 3 shows the parts of the skull that were then considered for manual landmarking using the output from landvR.

To investigate the landmarks of highest variation (and thus potential candidates for manual placement) we extract the 'radii' which is the radius per landmark for each specimen and '`radii_mean`' which is the mean radius per landmark. An example is provided below. Details are provided on Github (https://github.com/EllenJCoombs/Quantifying_asymmetry). An example of the results you can obtain using the below code are shown in Table 1. Much more can be done with these results should the user wish to investigate and visualise mean shapes and Procrustes distance, to name just two possibilities. See Guillerme and Weisbecker (2019) for further code and visualisations.

```
########################################
#                                      #
#   quantifying the level of asymmetry   #
#                                      #
########################################

#load packages and define model inputs

library(landvR)
N=123 #number of total landmarks
nfixed = 66 #number of fixed landmarks
specs = 157 #number of specimens
k = 3 #number of dimensions in the matrix
colfunc <- colorRampPalette(c("red", "yellow", "white")) #create colour function for visualising
landmarks
colfunc(10) #choose number of increments for colour scale



#make the array for analyses:
all_combined = array(dim=c(N,3,specs)) #3 is the columns of data we need (radii, azimuth, polar)

#manual_data is the fully landmarked skull (reference data)
#mirrored_data is the half-landmarked skull that has been mirrored

#calculate the coordinates.differences between these data sets (i.e. how much the landmarks move
between the manually placed landmarks and the mirrored landmarks)

i=1
for (i in 1:specs)
{
  all_differences <- coordinates.difference(coordinates = mirrored_data[,,i],
                                            reference = manual_data[,,i],
                                            type = "spherical",
                                            rounding = 9)

  all_combined[,,i]=all_differences[[1]]

  i=i+1
}


#landmarks 1:66 (nfixed) in this example are fixed and therefore have the value of zero
all_combined[1:nfixed, 1:k, 1:specs] <- c(0.000000, 0.000000, 0.000000)

#save output if desired using: write.csv(all_combined, file = 'all_combined.csv')

radii=all_combined[,1,] #radius per landmark for each specimen (second column of whole dataset with
just the radii [,1,])

radii_mean=apply(radii, c(1), mean) #c(1) look at the first column - the radii
#radii_mean is a mean radius value per landmark

#save radii and radii_mean as .csv files for further analyses

#example
#looking at the average radii compared to specimen 21 (or choose an average specimen if preferred)
get.col.spectrum <- landvR::procrustes.var.plot(manual_data[,,21], mirrored_data[,,21], col.val =
radii_mean, col = colfunc)
```

433 [Snippet on previous page]

434 **Code snippet 1**: Extracting the radii and average radii for each specimen using the landvR
435 package

436

437 [Table on next page]

438 **Table 1.** An example of the numerical outputs from landvR that help to inform areas of
439 asymmetry in the skull or chosen morphology. Shown are the five landmarks with the
440 greatest variation across the cranium for odontocetes in this study. $\bar{x}\rho_{land}$ is the average sum
441 radii per landmark. Skull shown is *Monodon monoceros* (USNM 267959).

442

443

444

445

446

Average asymmetry in the skull ($\bar{x}\rho$)	1st highest landmark of variation		2nd highest landmark of variation		3rd highest landmark of variation		4th highest landmark of variation		5th highest landmark of variation		Specimen showing top 5 landmarks (red)
	Landmark description	$\bar{x}\rho_{land}$	Landmark description	$\bar{x}\rho_{land}$	Landmark description	$\bar{x}\rho_{land}$	Landmark description	$\bar{x}\rho_{land}$	Landmark description	$\bar{x}\rho_{land}$	
0.245	**L71:** Posterior dorsal premaxilla	0.013	**L74:** Dorsal medial maxilla (suture with nasal and premaxilla)	0.011	**L68:** Posterior lateral corner of nasal	0.010	**L121:** Posterior point of nasal	0.009	**L75:** Nasal-frontal-maxilla suture (posterior medial maxilla)	0.009	

447

448

Step 4: Informing the curve protocol – which curves to manually place

For this data set, the top landmarks of variation were concentrated in the nasals, frontal, premaxilla, and maxilla (Fig. 3, Table 1). Asymmetry was also found in the orbit, lateral process of the maxilla, and the tip of the rostrum (Fig. 3 d-f). This informs our protocol for manually placing landmarks and curves on these bones, instead of mirroring. It also informs the landmarks and curves which can be mirrored, i.e., those that showed little asymmetry (pale yellow) such as the ventral and posterior of the skull in this example. Curves are then manually placed on one side of the skull for symmetrical structures (as is standard in bilaterally symmetrical specimens), with the addition of manual placement of curves on both sides of the face (maxilla, premaxilla, nasals, and frontal) to capture the morphology of asymmetric bones (Fig. 4). See Supporting Information; Table S3 for curve information.

See the methods section for infromation on resampling and sliding curves. This step is not specific to the asymmetric protocol that we address in this study but would be carried out at this stage, before mirroring curves.

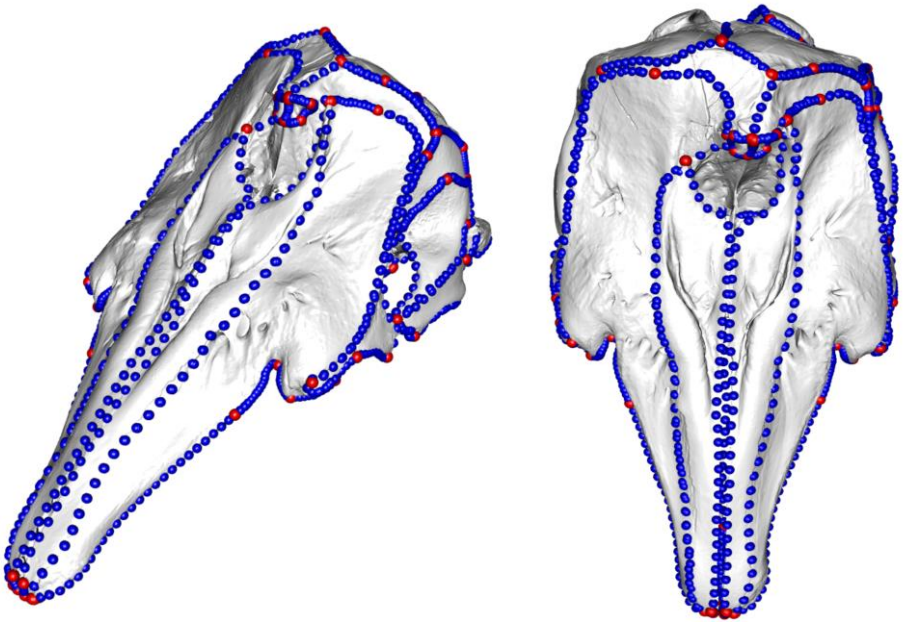

OBLIQUE DORSAL

Fig. 4. Curves and landmarks manually placed on the asymmetric cetacean face. Note the asymmetry in the posterior of the skull near the nasal. The manual placement of landmarks on the right hand side (RHS) of the skull are selected based on the results from landvR (Table 1, Fig. 3). Note the RHS posterior and the ventral skull are not shown with curves here because these are bilaterally symmetrical parts of the morphology (smaller radii values from landvR on the posterior and ventral of the skull) and thus landmarks and semi-landmark curves can be computer mirrored onto these sections (see Fig. 5 for full skull details). The skull on the left is shown in oblique view, the skull on the right is shown in dorsal view. Specimen shown is *Delphinapterus leucas* (USNM 305071).

Step 5: Placing landmarks and semi-landmarks on asymmetrical specimens

We use the results from landvR to determine which of the bones in the skull were asymmetric and thus requiring manual landmarking and which could be reliably placed by mirroring bilaterally symmetric landmarks across the skull midline. For the asymmetric specimens, we placed 57 landmarks on the LHS of the skull and nine landmarks on the midline. We mirrored 33 landmarks to symmetrical bones on the right-hand side (RHS) of the skull and we manually placed 24 landmarks on asymmetric bones on the RHS of the skull. We manually placed 60 curves using the 'curve' option in Checkpoint, on the sutures between bones on the LHS of the skull and four curves on the midline (Fig. 5). We manually placed 21 curves on asymmetrical bones (the face) on the RHS, mostly concentrated in the nasals, dorsal premaxilla, dorsal maxilla, orbit and rostrum, and the rest were computer-mirrored from the LHS (Fig. 5). Curves should then be resampled and slid (see Methods).

Code snippet 2 shows how to mirror bilaterally symmetrical curves only, whilst leaving manually placed (asymmetric) curves untouched. This results in manually placed asymmetric curves and computer mirrored bilaterally symmetrical curves being combined to cover the entire skull or morphology (Fig. 5). Using this method (code snippet 2) ensures that both bilaterally symmetrical specimens and asymmetric specimens (for example if specimens in the sample, e.g., a specific species, sex, or developmental stage have asymmetry, but other specimens do not) can still be compared in the same analyses as the number and location of landmarks and semi-landmark curves are identical, *only the method of placement is different*.

```
########################################
#                                      #
#   landmarking asymmetrical specimens   #
#                                      #
########################################

library(rgl)
library(paleomorph)
library(SURGE)

#import .csv defining curves
curve_table <- read_csv('new curves.csv')
my_curves <- create_curve_info(curve_table, n_fixed = 123) #define fixed curves


#slidedlms is resampled, slid landmarks with missing landmarks and variably present bones corrected
(see github for full code and 'side notes' section of methods)

#midline landmarks (anchor points via which landmarks are mirrored) in this example:
midline <-as.integer(c(38,40,48,49,51,54,55,56,61,1114,1115))

slidedlms <- Shape_data_with_bilats #see above
#define the curves and landmarks on each side
left.curves<-c(1:64)
left.lm <- c(1:37,39,41:47,50,52,53,57:60,62:66)
right.lm <- c(120,121,67:82,122,123,83:119)
right.curves <- c(65:85)
left.curve.list<-unlist(my_curves$Curve.in[left.curves])
right.curve.list<-unlist(my_curves$Curve.in[right.curves])
leftside<-c(left.lm,left.curve.list)
rightside<-c(right.lm, right.curve.list)
num.missing<-(length(leftside)-length(rightside))
blanks<-c((dim(slidedlms)[1]+1):(dim(slidedlms)[1]+num.missing))#to fill in blanks from one row past
the last current point, for the number of rows needed (num.missing)
rightside<-c(rightside,blanks)
add_col_or_row = function(x, n = 1, add_col = T, fill = 0)
{
  m1 = matrix(x, ncol = if(add_col) nrow(x) * ncol(x) else nrow(x), byrow = T)
  m2 = matrix(fill, nrow = if(add_col) dim(x)[3] else prod(dim(x)[-1]),
              ncol = if(add_col) nrow(x) * n else n)
  array(t(cbind(m1, m2)),
        c(nrow(x) + ((!add_col) * n), ncol(x) + (add_col * n), dim(x)[3]))
}
specimens<-add_col_or_row(slidedlms,n=num.missing,add_col=FALSE,fill=NA)
dimnames(specimens)[3]<-dimnames(slidedlms)[3] #make sure the specimens match up
bilats<-cbind(leftside,rightside) #bind the left and the right side
newarray<-mirrorfill(specimens,l1=midline,l2=bilats) #newarray = final, correctly mirrored landmarks
dimnames(newarray)[3]<-dimnames(slidedlms)[3] #make sure the specimens match up

#plot how the mirrored landmarks look
open3d();
spheres3d(newarray[,,3],radius=1.5) #plot whole skull to check asymmetric curve and symmetric curve
placement
spheres3d(newarray[bilats[,1],,1],col='red',radius = 1.5) #plot left side
spheres3d(newarray[bilats[,2],,1],col='blue',radius = 1.5) #plot right side
spheres3d(newarray[midline,,1], col = 'yellow', radius = 1.5) #plot midline
```

Code snippet 2: Code for mirroring bilaterally symmetrical curves alongside manually placed asymmetric curves. Complete code for mirroring symmetrical specimens is available at: https://github.com/EllenJCoombs/Quantifying_asymmetry

Results

Landmark and curve placement on asymmetrical specimens

Once these steps are followed, the user will have quantified where asymmetry exists in the specimen(s) and created a curve protocol that not only captures asymmetry in the structure or specimen but also accounts for any bilateral symmetry if present in that same structure or in other specimens in the data set. Examples of successful placement of curves in asymmetric and symmetric specimens are shown here (Fig. 5-7).

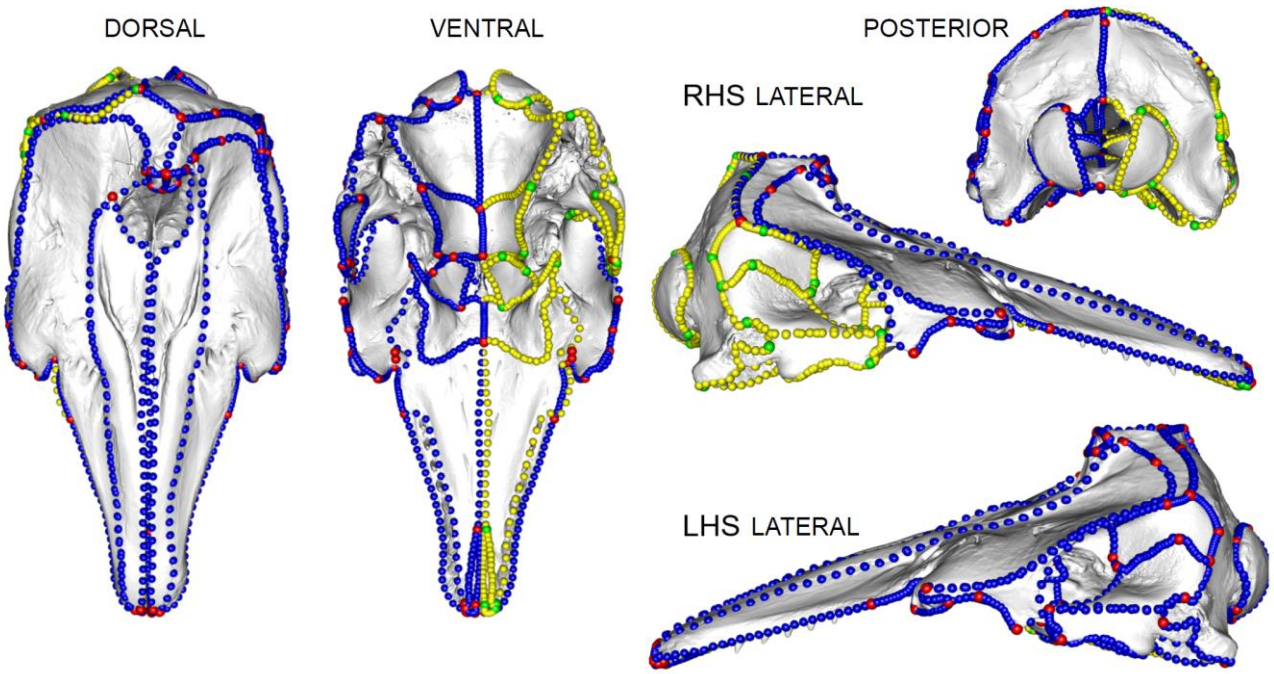

[Figure on previous page]

Fig. 5. Landmark configuration on an asymmetric skull. Red = manually placed landmarks on asymmetric bones, green = computer mirrored landmarks on symmetric bones, blue = manually placed curves (semi-landmarks) on asymmetric bones, yellow = computer mirrored curves (semi-landmarks) on symmetric bones. Specimen is *Delphinapterus leucas* (USNM 305071).

Additionally: Mirroring landmarks on bilaterally symmetrical specimens

On symmetrical specimens, here represented by the mysticetes (baleen whales) (see Fahlke and Hampe, 2015; Coombs et al., 2020) (Fig. 6), we placed 57 landmarks on the left-hand side (LHS) of the skull and nine landmarks on the midline. We placed 60 sliding semi-landmark curves on the sutures between bones on the LHS of the skull and four curves on the midline. These curves and landmarks were then mirrored (using the midline landmarks and curves as an anchor) using the `mirrorfill` function in the R package 'paleomorph' v.0.1.4 (See: https://github.com/EllenJCoombs/Quantifying_asymmetry). This method (see code snippet 2) ensures that both bilaterally symmetrical specimens and asymmetric specimens can be compared in the same analyses as landmark and curve numbers match between specimens. This results in a global landmark and curve configuration that is the same among specimens regardless of whether they are asymmetrical or not (Fig. 7).

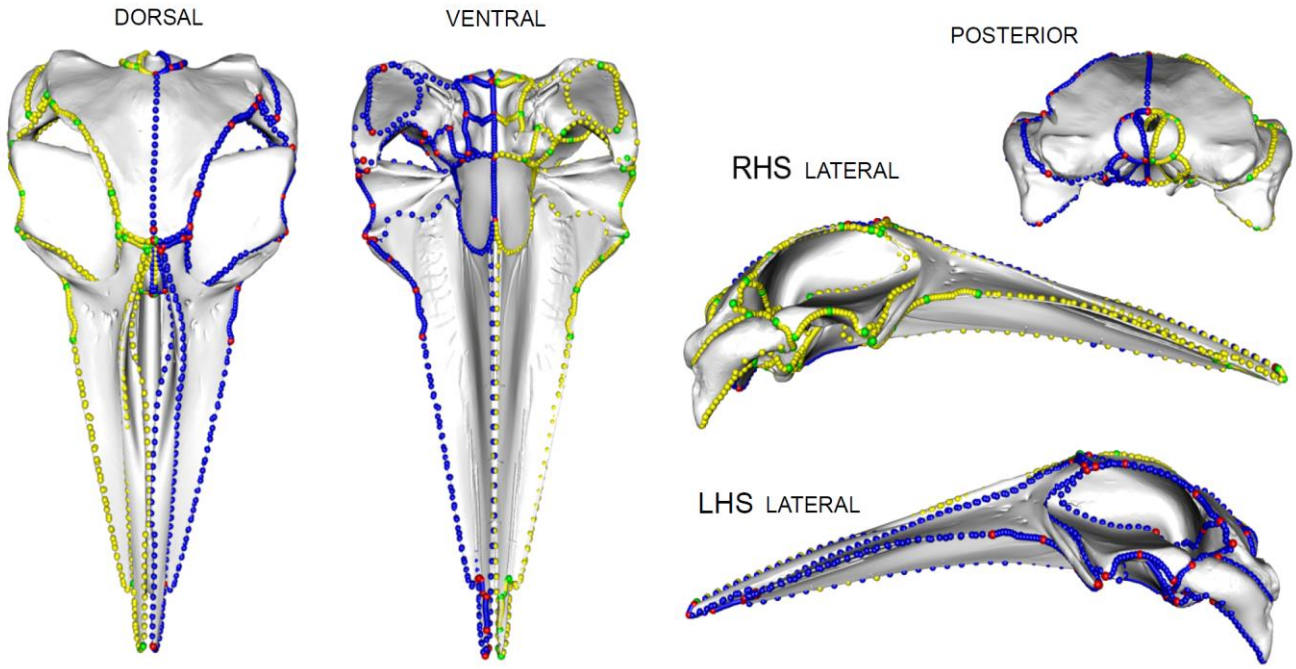

Fig.6. Landmark configuration on a symmetric skull. Landmark protocol for the symmetric mysticete. Red = manually placed landmarks, green = computer mirrored landmarks, blue = manually placed curves (semi-landmarks), yellow = computer mirrored curves (semi-landmarks). Specimen is *Balaenoptera acutorostrata* (NHM 1965.11.2.1).

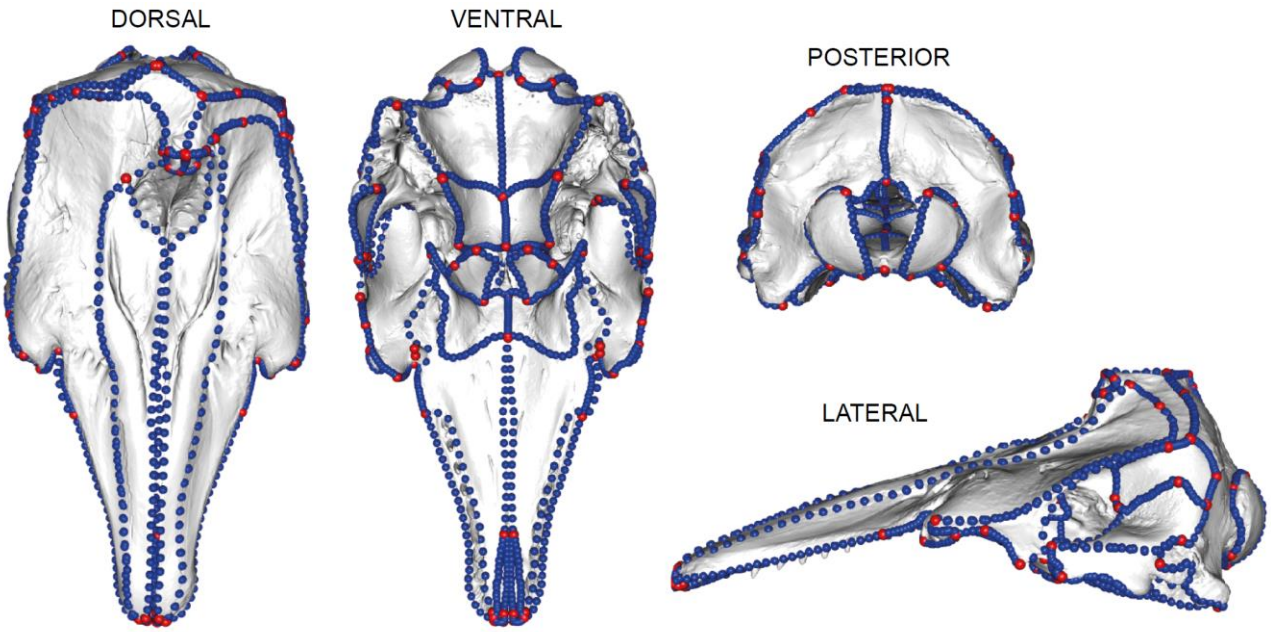

552

553

554 **Fig 7.** Final landmark and curve sliding semi-landmark placement on all skulls regardless of
555 asymmetry. The landmarks in red are type I and type II landmarks. The curves in blue define
556 outlines and margins of bones. There are 123 landmarks and 124 curves on this specimen.
557 Landmarks and curves shown on a beluga (*Delphinapterus leucas* (USNM 305071))
558 specimen. The methods of placement of these landmarks and curves are different
559 depending on whether the specimen is bilaterally symmetrical or asymmetrical; however, the
560 finished result (i.e., number of landmarks and curves and placement on bones) is uniform
561 across all specimens so that morphology is comparable.

562

563 Some odontocetes, such as phocoenids show little asymmetry in the skull (Cranford
564 et al., 1996; Marx et al., 2016). However, others, particularly highly asymmetrical
565 specimens such as the kogiids and physeteroids could be misrepresented in the
566 morphospace when using computer landmarks. In the example below we see that
567 asymmetric species (circled; Fig. 8) do shift in morphospace position if landmarks
568 are mirrored or manually placed. This is particularly evident in asymmetric

569 specimens such as monodontids, kogiids (Ness, 1967), and Physeteroidea (Coombs
570 et al., 2020).

571

572

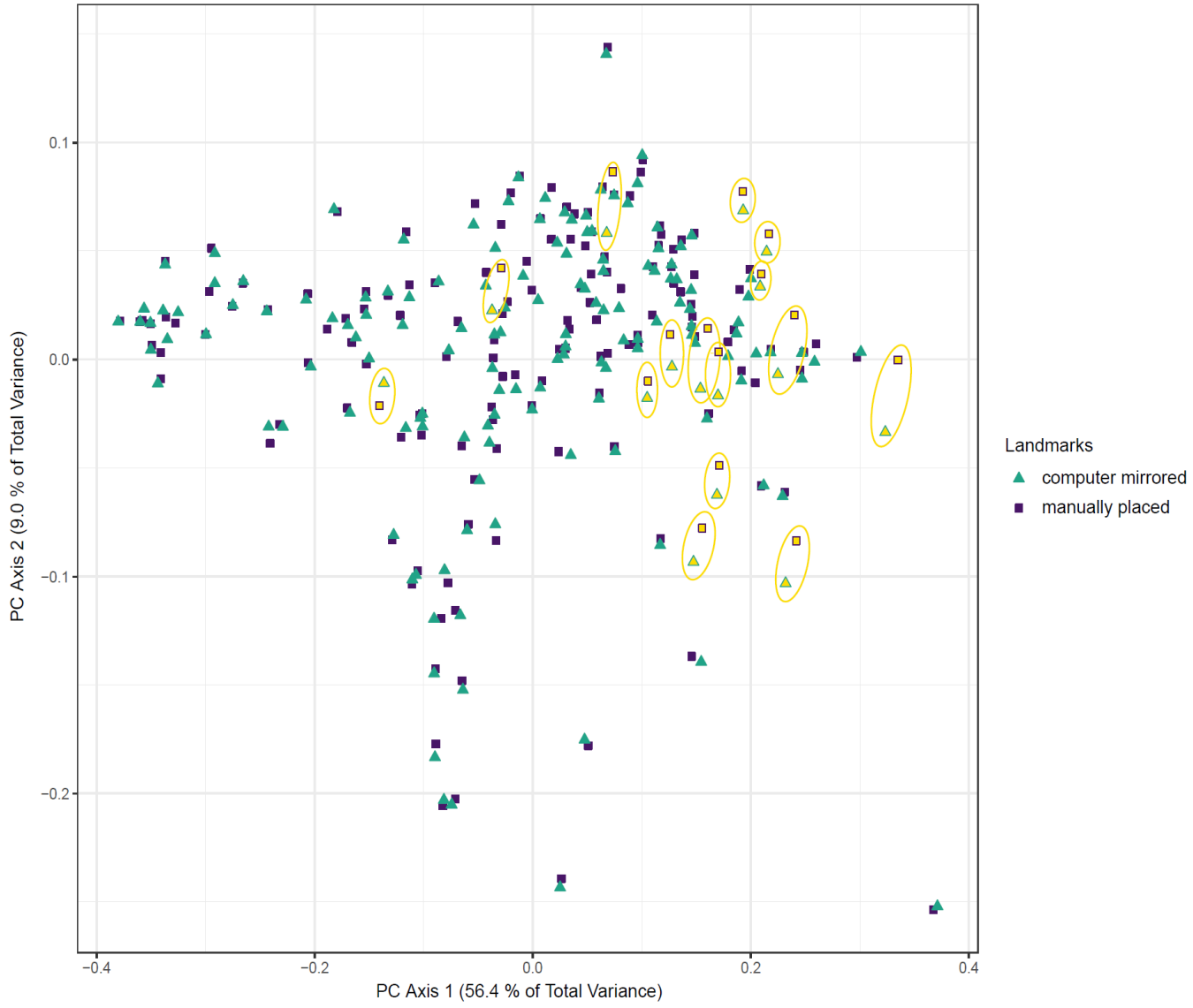

573

574

575

576

[Figure on previous page]

Fig. 8. An example of how specimens with some asymmetry (here concentrated in the naso-facial region of the skull) will sit in the morphospace when landmarked manually or using computer mirrored landmarks. The specimens with the greatest difference between their computer mirrored landmarks and manually placed landmarks (circled in yellow) are those with higher asymmetry. Morphospace of 157 odontocete skulls with landmark and semi-landmarks over the entirety of the skull (both asymmetric and symmetric bones).

Finally, for this specific data set, landmarking a skull using the method presented here took the researcher around a third less time than manually landmarking the whole skull.

Discussion

Directional asymmetry in organisms is a fascinating phenomenon but can complicate data collection by making automated mirroring of morphometric data inappropriate. Methods such as mirroring landmarks is a standard technique used for bilaterally symmetrical specimens (Gunz et al., 2009; Cardini et al., 2010; Gunz and Mitteroecker, 2013) which provide an accurate quantification of morphology whilst reducing the time needed to landmark the entire surface of the skull (Bardua et al., 2019a). However, while this is a suitable technique for bilaterally symmetrical structures, it may misrepresent asymmetric structures. Further, it can be difficult to detect asymmetry ‘by eye’ and then landmark a specimen as such based on a visual interpretation. Not accurately quantifying asymmetry in the initial stages could result in asymmetry being missed or perhaps even overrepresented. Here we offer a practical method to accurately quantify the morphology but also minimise the time by about a third (in this example data set) to manually landmark the entire specimen.

Natural, directional asymmetry occurs when one side of the structure is consistently different (e.g., in size or shape) (Graham et al., 1993; Parés-Casanova, 2020). Directional asymmetry is recorded in many specimens, from algae and leaf blades to corals, turtles, and birds. In some taxa, asymmetry can be genus or even sex specific, for example, male speckled wood butterflies (*Pararge aegeria*) have directional asymmetry in the fore and hindwing and forewing width (Windig and Nylin, 1999) and in cetaceans, families such as the monodontids and the kogiids have more naso-facial asymmetry than families such as the delphinids (Ness, 1967). It is therefore useful to have a protocol that can be used to capture morphology in both asymmetric and symmetric specimens that are to be analysed together. This protocol results in a global landmark and curve configuration that is the same among specimens regardless of whether they are asymmetrical or not (Fig. 6; Fig. 7).

This protocol provides a substantial increase in data collection speed. The time-consuming nature of digitising 3D landmark and semi-landmark data can impose limitations on sampling in resource-limited research projects. This has led some researchers to seek automated (Boyer et al., 2015a; 2015b) or semi-automated (Schlager et al. 2019) approaches to geometric morphometrics, but these methods are not applicable to all morphologies or hypotheses. We estimate that using the method presented here (i.e., manually semi-landmarking asymmetric bones and mirroring semi-landmarks for bilaterally symmetric bones only) reduces per-specimen processing time by about one third compared to applying semi-landmark curves to the whole skull. Gains in digitisation speed will be specific to the data set in question, for example, taxa with more asymmetry would require more manual landmarking and thus an increased time investment to accurately capture the asymmetric morphology.

A time effective method is desirable to any researcher but most important is the accurate representation of a specimen and its morphology. This method helps to first quantify any asymmetry in the morphology, and then to accurately represent it. In the example shown (Fig. 8) this goes as follows; computer mirrored landmarks and curves and manually placed landmarks and curves are placed on odontocete skulls to observe the difference that incorrectly placed landmarks can have on reporting morphology. Importantly, the difference between manual and mirrored specimens can be as great as the difference between species (Fig. 8) and thus has the potential to mislead downstream analyses. We find that the incorrect placing of specimens in the morphospace (via incorrect landmarking) can place specimens as far from their true morphology (if correctly landmarked) as from other species. This in turn could influence results that may be looking at, for example, ecological influences on morphology, such as species-specific diet, habitat, or other ecological factors. It is therefore central to ascertain which specimens in a sample could be misrepresented by mirroring of landmarks.

Limitations

Finally, there are some limitations to this exploratory approach. Firstly, the method is most likely useful for studies where measurement error is small compared to biological variation, for example, macroevolutionary studies, interspecific studies, ontogenetic studies, and studies of sexual dimorphism. Variation in intraspecific studies may be small and difficult to quantify using this method. That said, we still recommend quantifying asymmetry in intraspecific cohorts and on specimens with assumed bilateral symmetry if only to a) confirm the latter and thus support the

mirroring of landmarks from one half of the morphology to the other, or b) highlight any deformation in specimens, especially fossils. Secondly, an understanding of the specimen's morphology is desirable to interpreting the outputs from landvR, for example, it is useful to know whether landmarks that show up in hotter colours (red, dark orange) are reflective of the biology or an artefact of deformation. An in-depth anatomical knowledge of study specimens is not a prerequisite, but we do recommend considering asymmetric landmarks carefully to ascertain whether any observed asymmetry is likely biological or deformational.

The code for these analyses is available at: https://github.com/EllenJCoombs/Quantifying_asymmetry. The code relies heavily on functions available in the SURGE package (Felice, 2020) and the Paleomorph package (Lucas and Goswami, 2017). Due to advances in coding and imaging technologies, we anticipate continual updates to these methods and welcome user suggestions and contributions.

Acknowledgements

We would like to thank Anjali Goswami for her comments on drafts of this manuscript and Thomas Guillerme for help and assistance with the landvR package. Thanks also go to the many curators and museum staff who helped EJC collect scan data.

Author contributions

EJC conceived the idea. EJC and RNF designed the methodology. EJC collected and analysed the data. RNF compiled code. Both authors contributed critically to the drafts and gave final approval for publication.

Conflicts of interest

The authors declare no conflicts of interest.

Funding

EJC was funded by the London Natural Environment Research Council Doctoral Training Partnership (London NERC DTP) training grant NE/L002485/1.

Data availability

All data and code are freely available and are stored at:
https://github.com/EllenJCoombs/Quantifying_asymmetry

Supporting information

Additional supporting information may be found in the Supporting Information section.

699 **References**

700 Adams, D.C., Collyer, M.L., Kaliontzopoulou, A. (2019) Geomorph: software for geometric
701 morphometric analyses. In: R package version 3.1.0. See https://cran.r-
702 project.org/package=geomorph

703 Adams, D.C., Rohlf, F.J., Slice, D.E. (2013) A field comes of age: geometric morphometrics
704 in the 21st century. Hystrix24:7–14.

705 Auerbach, B. M., and Ruff, C. B. (2006). Limb bone bilateral asymmetry: variability and
706 commonality among modern humans. Journal of Human Evolution, 50(2), 203–218.
707 https://doi.org/10.1016/J.JHEVOL.2005.09.004

708 Bahadur B (2019). Krishnamurthy KV, Ghose M, John Adam S (eds) Asymmetry in Plants:
709 biology of handedness, The Concepts of Handedness, Asymmetry, Chirality, Spirality, and
710 Helicity in Taylor and Francis Publisher, pp. 1–14. CRC Press

711 Bardua. C., Felice, R.N., Watanabe. A, Fabre, A-C, Goswami. A (2019a). A Practical Guide
712 to Sliding and Surface Semilandmarks in Morphometric Analyses, Integrative Organismal
713 Biology, Volume 1, Issue 1, obz016, https://doi.org/10.1093/iob/obz016

714 Bardua, C., Wilkinson, W., Gower, D.J., Sherratt. E., and Goswami, A. (2019b)
715 Morphological evolution and modularity of the caecilian skull. BMC Evolutionary Biology 19
716 (1), 30.

717 Black, C.R and Berendzen, P.B. (2020) Shared ecological traits influence shape of the
718 skeleton in flatfishes (Pleuronectiformes). PeerJ 8, e8919. https://doi.org/10.7717/peerj.8919

719 Bookstein, F.L. (1997) Landmark methods for forms without landmarks: morphometrics of
720 group differences in outline shape. Med Image Anal1:225–43.

721 Bookstein, F.L. (1991). Morphometric tools for landmark data: geometry and biology.
722 Cambridge: Cambridge University Press.

723 Botton-Divet, L., Cornette, R., Fabre A-C., Herrel, A., Houssaye, A. (2016) Morphological
724 analysis of long bones in semi-aquatic mustelids and their terrestrial relatives. Integr Comp
725 Biol 56:1298–309. https://doi.org/10.1093/icb/icw124

726 Boyer DM, Puente J, Gladman JT, Glynn C, Muhkerjee S, Yapunich

727 GS, Daubechies I. (2015a) A new fully automated approach for aligning

728 and comparing shapes. Anat Rec 298:249–276.

729 Boyer DM, Winchester JM, Glynn C, Puente J. (2015b) Detailed Anatomical Orientations for
730 Certain Types of Morphometric Measurements Can Be Determined Automatically With
731 Geometric Algorithms. Anat Rec.

732 Bravi R, Benitez HA (2013) Left-right asymmetries and shape analysis on Ceroglossus
733 chilensis (Coleoptera: Carabidae). Acta Oecologica-International Journal of Ecology 52: 57–
734 62.

735 Cardini, A. (2016a). Left, right or both? Estimating and improving accuracy of one-side-only
736 geometric morphometric analyses of cranial variation. J Zool Syst Evol Res55:1–10.

737 Cardini, A. (2016b). Lost in the other half: improving accuracy in geometric morphometric
738 analyses of one side of bilaterally symmetric structures. Syst Biol65:1096–106.
739 https://doi.org/10.1093/sysbio/syw043

740 Cardini, A., Felizola Diniz Filho, J.A, Polly, D.P., Elton, S. (2010) Biogeographic analysis
741 using geometric morphometrics: clines in skull size and shape in a widespread African
742 arboreal monkey. In: Lecture Notes in Earth Sciences; p. 191–217.

743 Churchill, M., Geisler, J., Beatty, B., Goswami, A. (2018) Evolution of cranial telescoping in
744 echolocating whales (Cetacea: Odontoceti), evolution. Soc Stud Evol. 72(5):1092–108.
745 https://doi.org/10.1111/evo.13480

746 Coombs, E. J., Clavel, J., Park, T., Churchill, M., & Goswami, A. (2020). Wonky whales: the
747 evolution of cranial asymmetry in cetaceans. BMC Biology 2020 18:1, 18(1), 1–24.
748 https://doi.org/10.1186/S12915-020-00805-4

749 Cooney, C. R., Bright, J. A., Capp, E. J. R., Chira, A. M., Hughes, E. C., Moody, C. J. A.,
750 Nouri, L. O., Varley, Z. K., & Thomas, G. H. (2017). Mega-evolutionary dynamics of the
751 adaptive radiation of birds. Nature, 542(7641), 344. https://doi.org/10.1038/NATURE21074

752 Cranford, T. W., Amundin, M., & Norris, K. S. (1996). Functional morphology and homology
753 in the odontocete nasal complex: Implications for sound generation. Journal of Morphology,
754 228, 223–228.

755 Davies, T.G., Rahman, I.A., Lautenschlager, S., Cunningham, J.A., Asher, R.J., Barrett,
756 P.M., Bates, K.T., Bengtson, S., Benson, R.B.J., Boyer, D.M., Braga, J. et al. (2017). Open
757 data and digital morphology. Proc R Soc B Biol Sci 284:20170194.
758 https://doi.org/10.1098/rspb.2017.0194

759 Dumont, M., Wall, C.E., Botton-Divet, L., Goswami, A., Peigné, S., Fabre, A-C. (2016) Do
760 functional demands associated with locomotor habitat, diet, and activity pattern drive skull

761 shape evolution in musteloid carnivorans? Biological Journal of the Linnean Society, Volume
762 117, Issue 4, April 2016, Pages 858–878, https://doi.org/10.1111/bij.12719

763 Evans, K. M., Larouche, O., Watson, S.-J., Farina, S., Laura Habegger, M., & Friedman, M.
764 (2021) Integration drives rapid phenotypic evolution in flatfishes. PNAS. 118 (18)
765 e2101330118; https://doi.org/10.1073/pnas.2101330118

766 Fahlke, J.M, Hampe, O. (2015) Cranial symmetry in baleen whales (Cetacea, Mysticeti) and
767 the occurrence of cranial asymmetry throughout cetacean evolution. Naturwissenschaften.
768 2015;102(9-10):58.

769 Fahlke, J.M., Gingerich, P.D., Welsh, R.C., Wood, A.R. (2011) Cranial asymmetry in Eocene
770 archaeocete whales and the evolution of directional hearing in water. Proc Natl Acad Sci U S
771 A. 108(35):14545–8. https://doi.org/10.1073/pnas.1108927108

772 Falk, D., Pyne, L., Helmkamp, R. C., DeRousseau, C. J. (1988). Directional asymmetry in
773 the forelimb of M. mulatta. American Journal of Physical Anthropology, 77, 1-6.

774 Felice, R.N (2020). SURGE: SURface Geometric morphometrics for Everyone. R package
775 version 0.1.0. https://github.com/rnfelice/SURGE/

776 Felice, R.N and Goswami. A. (2018) Developmental origins of mosaic evolution in the avian
777 cranium. Proceedings of the National Academy of Sciences, USA, 115: 555-560.
778 https://doi.org/10.1073/pnas.1716437115

779 Galatius, A. (2006). Taxonomy of dolphins Delphinus and Tursiops spp. View project Marine
780 mammal management in light of eco-tourism View project Bilateral Directional Asymmetry of
781 the Appendicular Skeleton of the White-Beaked Dolphin (*Lagenorhynchus albirostris*).
782 https://doi.org/10.1578/AM.32.2.2006.232

783 Galatius, A. and Jespersen, Å (2005). Bilateral Directional Asymmetry Of The Appendicular
784 Skeleton Of The Harbor Porpoise (*Phocoena Phocoena*). Marine Mammal Science, 21(3),
785 401–410. https://doi.org/10.1111/J.1748-7692.2005.TB01240.X

786 Goswami, A., Watanabe, A., Felice, R.N., Bardua, C., Fabre, A-C., and Polly, P.D. (2019).
787 High-density morphometric analysis of shape and integration: the good, the bad, and the
788 not-really-a-problem. Integrative and Comparative Biology, 59: 669–683.
789 https://doi.org/10.1093/icb/icz120

790 Graham, J. H., Carl Freeman, D., & Emlen, J. M. (1993). Antisymmetry, directional
791 asymmetry, and dynamic morphogenesis. Genetica, 89(9), 121–137.

792 Guillerme, T., Weisbecker, V. landvR: tools for measuring landmark position variation:
793 Zenodo; (2019). https://doi.org/10.5281/zenodo.2620785

794 Gunz, P. and Mitteroecker, P. (2013) Semilandmarks: a method for quantifying curves and
795 surfaces. Hystrix. 24:103–9.

796 Gunz, P., Mitteroecker, P., Bookstein, F.L. (2005) Chapter three: semilandmarks in three
797 dimensions. In: Slice DE, editor. Modern morphometrics in physical anthropology. New York:
798 Kluwer Academic/Plenum. p. 73–98.

799 Gunz, P., Mitteroecker, P., Neubauer, S., Weber, G.W, et al. (2009) Principles for the virtual
800 reconstruction of hominin crania. J Hum Evol. 57(1):48–62.

801 Heyning, J.E, and Mead, J.G. Evolution of the nasal anatomy of cetaceans, in sensory
802 abilities of cetaceans. (1990) US: Springer, p. 67–79.

803 Kharlamova, A. V., Trut, L. N., Chase, K., Kukekova, A. V., & Lark, K. G. (2010). Directional
804 asymmetry in the limbs, skull and pelvis of the silver fox (V. vulpes). Journal of Morphology,
805 271(12), 1501–1508. https://doi.org/10.1002/JMOR.10890

806 Klingenberg, C. P., McIntyre, G. S., Zaklan, S. D. (1998) Leftright asymmetry of fly wings
807 and the evolution of body axes. Proc. R. Soc. Lond. B Biol. Sci. 265:1255–1259.

808 Klingenberg, C. P., & McIntyre, G. S. (1998a). Geometric morphometrics of developmental
809 instability: Analyzing patterns of fluctuating asymmetry with Procrustes methods. Evolution;
810 International Journal of Organic Evolution, 52(3), 363–1375.

811 Klingenberg C. P and McIntyre G. S. (1998b) Geometric morphometrics of developmental
812 instability: analyzing patterns of fluctuating asymmetry with Procrustes methods. Evolution,
813 52: 1363-1375.

814 Klingenberg, C. P., Barluenga, M., Meyer, A. (2002). Shape analysis of symmetric
815 structures: quantifying variation among individuals and asymmetry. Evolution, 56(10), 1909–
816 1920.

817 Klingenberg, C.P. (2003) Developmental instability as a research tool: Using patterns of
818 fluctuating asymmetry to infer the develop- mental origins of morphological integration. In
819 Developmental Instability: Causes and Consequences; Polak, M., Ed.; Oxford Uni- versity
820 Press: New York, NY, USA.

821 Klingenberg CP (2015) Analyzing fluctuating asymmetry with geometric morphometrics:
822 concepts, methods, and applications. Symmetry 7:843–934

Krings, M., Castanhinha, R., Müller-Limberger, E., Wipfler, B., & Wagner, H. (2020). Ear asymmetry in Tengmalm's owl (*Aegolius funereus*): Two phases of asymmetrical development of the squamoso-occipital wing. Zoology, 141, 125814. https://doi.org/10.1016/J.ZOOL.2020.125814

Lawing, A. M., and Polly, P. D. (2010). Geometric morphometrics: recent applications to the study of evolution and development. J Zool280:1–7.

Levermann, N., Galatius, A., Ehlme, G., Rysgaard, S., & Born, E. W. (2003). Feeding behaviour of free-ranging walruses with notes on apparent dextrality of flipper use. BMC Ecology 3.

Lucas, T., and Goswami, A. (2017) Paleomorph: geometric morphometric tools for paleobiology. In: R package version 0.1.4 (https://CRAN.R-project.org/package=paleomorph); 2017.

Macleod, C.D., Reidenberg, J.S., Weller, M., Santos, M.B., et al. (2007) Breaking symmetry: the marine environment, prey size, and the evolution of asymmetry in cetacean skulls. Anat Rec. 290(6):539–45

Marx, F. G., Lambert, O., and Uhen, M. D. (2016). Cetacean paleobiology. Cetacean Paleobiology, 1–319.

Mitteroecker, P. and Gunz, P. (2009). Advances in Geometric Morphometrics. Evolutionary Biology. 36. 235-247. https://doi.org/10.1007/s11692-009-9055-x

Ness, A.R. (1967) A measure of asymmetry of the skulls of odontocete whales. J Zool. 153:209–21.

Norberg, R. Å. (2002) Independent evolution of outer ear asymmetry among five lineages; morphology, function and selection. I. Newton, R. Kavanagh, J. Olsen, I. Taylor (Eds.), Ecology and Conservation Of Owls, CSIRO Publishers, Clayton, Australia, pp. 329-342

Norberg, R. Å. Ocurrence and independent evolution of bilateral ear asymmetry in owls and implications on owl taxonomy. (1977) Philosophical Transactions of the Royal Society of London. B, Biological Sciences, 280(973), 375–408. https://doi.org/10.1098/rstb.1977.0116

Okumura, T., Utsuno, H., Kuroda, J., Gittenberger, E., Asami, T., & Matsuno, K. (2008). The Development and Evolution of Left-Right Asymmetry in Invertebrates: Lessons from Drosophila and Snails. Developmental Dynamics, 237, 3497–3515. https://doi.org/10.1002/dvdy.21788

854 Parés-Casanova, P.M (2020). Directional asymmetry in the yellow-bellied slider turtles
855 (Trachemys scripta scripta) (Schoepff 1792). Herpetol. Notes 2020, 13, 587–592.

856 Payne, R.S. (1971) Acoustic location of prey by barn owls (*Tyto alba*). J. Exp. Biol., 54
857 (1971), pp. 535-573

858 Pélabon, C., & Hansen, T. F. (2008). On the Adaptive Accuracy of Directional Asymmetry in
859 Insect Wing Size. Evolution, 62(11), 2855–2867.

860 Schlager. S, Jefferis. G, Ian. D, Schlager, M.S. Package 'Morpho' (2019) http://cran.r-
861 project.org/web/packages/Morpho/Morpho.pdf

862 Google ScholarThomas, K.N, Robison, B.H, Johnsen, S. (2017). Two eyes for two purposes:
863 in situ evidence for asymmetric vision in the cockeyed squids *Histioteuthis heteropsis* and
864 *Stigmatoteuthis dofleini*. Phil. Trans. R. Soc. B 372: 20160069.

865 Thompson, P. (1990) The bottlenose dolphin. Trends Ecol Evol. 5(11):390 Edited by
866 Leatherwood. S and Reeves. R. Elsevier Science.

867 Viacava P, Blomberg SP, Sansalone G, Phillips MJ, Guillerme T, Cameron SF, Wilson RS,
868 Weisbecker V. (2020) Skull shape of a widely distributed, endangered marsupial reveals little
869 evidence of local adaptation between fragmented populations. Ecol. Evol. 10, 9707–9720.
870 (doi:10.1002/ece3.6593)

871 Watanabe, A., Fabre, A-C, Felice, R.N., Maisano, J.A., Müller, J., Herrel, A., and Goswami,
872 A. (2019) Ecomorphological diversification in squamates from conserved pattern of cranial
873 integration. Proceedings of the National Academy of Sciences, USA, 116 (29), 14688-14697.

874 Weisbecker, V., Guillerme, T., Speck, C. et al. (2019) Individual variation of the masticatory
875 system dominates 3D skull shape in the herbivory-adapted marsupial wombats. Front Zool
876 16, 41 (2019). https://doi.org/10.1186/s12983-019-0338-5

877 Windig J. J and Nylin. S (1999). Adaptive wing asymmetry in males of the speckled wood
878 butterfly (*Pararge aegeria*)? *Proc. R. Soc. Lond. B.***266**1413–1418
879 http://doi.org/10.1098/rspb.1999.0795

880 Zelditch, M., Swiderski, D.L., Sheets, H.D., Fink, W.L (2004). Geometric morphometrics for
881 biologists: a primer. Boston: Elsevier Academic Press.

882

883